

MAREK KALBARCZYK\*, REMIGIUSZ MICHALCZEWSKI\*,  
WITOLD PIEKOSZEWSKI\*, MARIAN SZCZEREK\*

## **The correlation between 3D surface parameters of a ceramic element and the tribological characteristics in ceramic-polymer joints**

### Key - words

Ceramics for hip joint prosthesis, atomic force microscope (AFM), pin-on-flat testing machine, 3D surface parameters.

### Słowa kluczowe

Ceramiczne materiały na endoprotezy, mikroskop sił atomowych (AFM), tribotester typu trzpień-płytką, parametry chropowości powierzchni.

### Summary

The aim of the study was a correlation between the tribological characteristics of a lubricated ceramic-polymer friction joint and the 3D roughness parameters of ceramic body.

The tests of materials in reciprocating motion were performed by means of a pin-on-flat tribotester denoted as T-17. The ceramic plates with various roughness parameters which containing different concentration of  $ZrO_2$  and  $Al_2O_3$  rubbing against UHMWPE specimen were tested. The friction and wear in presence of Ringer solution were measured.

---

\* Institute for Sustainable Technologies – National Research Institute, Tribology Department ul. Pułaskiego 6/10, 26-600 Radom, Poland, phone: (48-48) 3614241, e-mail: marek.kalbarczyk@itee.radom.pl

An atomic force microscope (AFM) was employed for observation and 3D surface parameter measurement of the specimen surfaces with nanoscale precision before and after tests.

It was found that, in the case of ceramic-polymer friction joints working under reciprocating motion, the correlation between the friction coefficient and wear and roughness parameters exists. The friction coefficient and wear are lower for higher values of the roughness parameters of the ceramic plate.

The roughness of hard ceramics affects the process of polymer transfer. In the case of high rough surfaces, polymer material is smeared on the ceramic surface creating a thin polymer film. However, in the case of smooth ceramic surfaces, the strong adhesive bounds are created and some large particles of polymer are transferred to the ceramic surface. To summarise, the correlation between 3D surface parameters and tribological characteristics is also confirmed by the differences in the material transfer process.

## 1. Introduction

Currently endoprosthesis heads are mostly made of stainless steel and also of chromium, nickel, cobalt, and molybdenum alloys (e.g.: Vitalium, Co-Cr alloy) [1, 2]. The acetabular cups of prosthesis are usually manufactured from polymers (e.g. UHMWPE, PTFE) [2, 3, 4]. However, these endoprosthesis demonstrate insufficient durability, which causes the need of expensive replacement.

There are two main methods of increasing the durability of endoprosthesis currently being researched: new constructional solutions, e.g.: BHR system [4, 5, 6], selection of newer, more wear resistant materials, e.g.: Titanium alloys [7, 8, 9], or elements coated with modern antiwear coatings [8, 9].

Increasingly, endoprosthesis heads are produced from ceramic materials based on aluminium, zirconium, and yttrium [3, 4]. Ceramic materials reveal higher biocompatibility and higher wear resistance than the typical alloy materials. These ceramic materials are now a subject of much research [2, 4, 10].

The main problem occurring during the production of ceramic prosthesis heads is the treatment that aims at the achievement of the proper shape and low surface roughness [3, 4, 11]. The reduction in surface roughness is a method for the elimination of microscratching between the soft polymer and the hard ceramic. This process is extremely expensive and seems insufficiently justified.

Earlier research mostly indicated that, after exceeding the critical value of 3D surface parameters, the expensive process to attain the lowest surface roughness does not lead to an increase in the wear resistance of the lubricated friction joint [12]. Moreover, in this kind of friction joint, it is recommended to apply cross-section machining [13], which causes the load-carrying capacity to increase and the pressure inside the friction joint to decrease. This results in lowering of friction coefficient.

The aim of this paper was to investigate the influence of measured, in nanoscale, 3D surface roughness parameters on the tribological characteristics of lubricated ceramic-polymer couples. The analyses of the stereometry structure of the ceramic elements' surfaces were performed by means of an atomic force microscope.

## 2. Experimental details

The investigation of tribological characteristics were performed by means of a reciprocating pin-on-flat testing machine T-17, designed and produced in ITeE-PIB [14]. Using this device it is possible to perform tests according to ASTM 732-82 standard (and others) related to the tribological properties of materials for endoprosthesis. The friction couple consisted of a stationary pin pressed into a reciprocating plate.

The scheme and the view of the T-17 apparatus friction joint are shown in Fig. 1. The Ringer solution was used as a lubricant for these tests [15, 16].

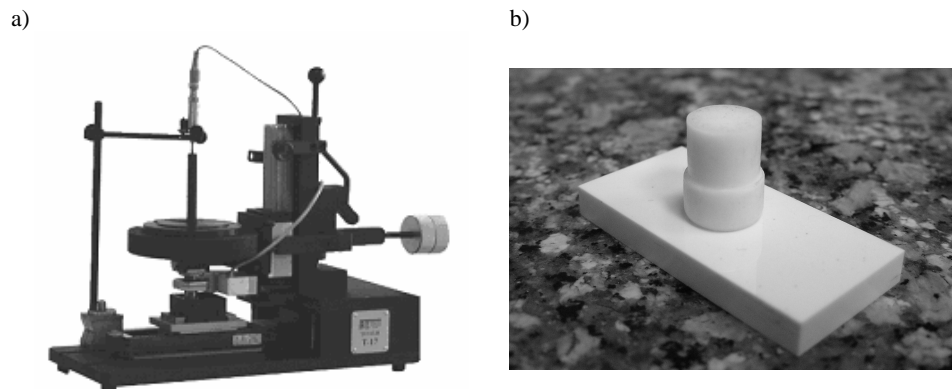


Fig. 1. T-17 pin-on-flat tribotester: a) tester, b) friction couple

Rys. 1. Tribotester typu trzpień-płytki T-17: a) fotografia, b) przykład badanego skojarzenia

For every friction couple, at least three tests were performed with the following parameters according to ASTM 732-82 standard:

- Reciprocating motion frequency: 1 cycle/s,
- Stroke: 25 mm,
- Number of cycles: 1 000 000,
- Unit pressure: 3,54 MPa,
- Lubricant temperature:  $37 \pm 1^\circ\text{C}$ .

The average value of the friction force and total wear were measured for every friction couple. The friction coefficient and the wear intensity were calculated from trend lines after the run-in period. The standard deviation of friction coefficient values was determined. From trend line equations of the wear intensity, the  $R^2$  parameter was calculated.

The pin was produced from UHMWPE, which is in common use for manufacturing endoprosthesis acetabular cups. The plate specimens were produced from ceramic materials destined for endoprosthesis heads. The shape and size of the pin and plate are shown in Fig. 2.

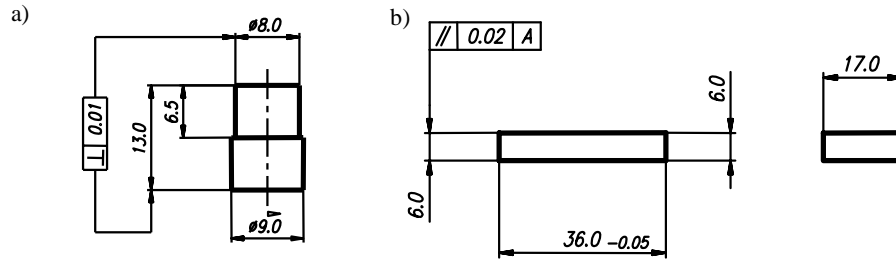


Fig. 2. Specimens: a) pin, b) plate  
Rys. 2. Badane próbki: a) trzpień, b) płytką

Specimens A, B, C, and D were composed from  $ZrO_2$  and  $Al_2O_3$ . The plates denoted as A and B were made in two various roughness versions and named as follows: A1, A2, B1, and B2. Number 1 was used for the surface that was exposed to a finishing treatment by means of an abrasive with higher grain size.

Considering very low roughness, the surface measurements conducted by means of a profilometer achieved very high errors. This was the result of mechanical filtration caused by the curvature radius of the gauge needle.

The three-dimensional surface analysis and three-dimensional roughness parameter determination (Table 1) were conducted by means of an atomic force microscope – AFM [17]. The size of the investigated surface was  $50 \mu m \times 50 \mu m$ , and the scanning resolution was 600 lines. All measurements were made using intermittent mode described as Wave Mode.

Table 1. 3D surface parameters measured by means of AFM  
Tabela 1. Parametry powierzchni mierzone przy użyciu AFM

Parameter	Symbol	Equation
Average Roughness	$R_a$	$R_a = \frac{1}{N} \sum_{n=1}^{n=N}  z_n - \bar{z} $
Root Mean Square	RMS	$R_q = \sqrt{\frac{1}{N} \sum_{n=1}^{n=N} (z_n - \bar{z})^2}$
Average height	A	$\bar{z} = \frac{1}{N} \sum_{n=1}^{n=N} z_n$
Average height difference	$R_z$	$R_z = \frac{1}{5} \left[ \sum_{i=1}^5  R_{pi}  + \sum_{i=1}^5  R_{vi}  \right]$
Skewness	S	$R_{sk} = \frac{1}{NR_q^3} \sum_{n=1}^{n=N} (z_n - \bar{z})^3$
Kurtosis	K	$R_{ku} = \frac{1}{NR_q^4} \sum_{n=1}^{n=N} (z_n - \bar{z})^4 - 3$

### 3. Tribological results

As a result of tribological research performed on T-17 tester, the curves of friction force and total wear were obtained for UHMWPE with the following ceramic specimens: A1, A2, B1, B2, C, D. On the basis of obtained charts, the average values of the friction coefficient and wear intensity were determined. The results were put in Table 2, in ascending order of the total friction couple wear intensity. In the case of ceramic-polymer pairs, mainly the wear of the polymer material takes place.

Table 2. The average values ( $\bar{z}$ ) and standard deviation ( $\sigma$ ) of friction coefficient and average values ( $\bar{z}$ ) and adjustment coefficient ( $R^2$ ) of wear intensity of investigated friction pairs  
Tabela 2. Wartości średnie ( $\bar{z}$ ) oraz odchylenia standardowe ( $\sigma$ ) współczynnika tarcia i wartości średnie intensywności zużywania ( $\bar{z}$ ) oraz współczynniki dopasowania ( $R^2$ ) dla badanych skojarzeń

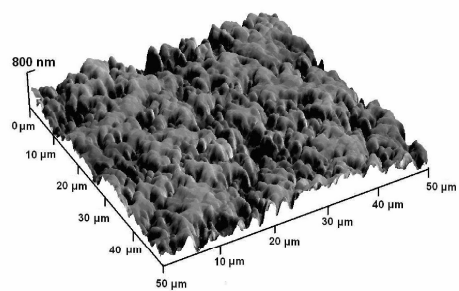
Specimen symbol	The friction coefficient		Wear intensity [ $\mu\text{m} / 1$ million cycles]	
	$\bar{z}$	$\sigma$	$\bar{z}$	$R^2$
A1	0.057	0.003	14.72	0.84
B1	0.090	0.016	31.17	0.96
C	0.098	0.024	33.02	0.96
A2	0.110	0.031	47.70	0.95
D	0.115	0.030	66.07	0.99
B2	0.130	0.027	72.30	0.99

The lowest friction coefficient and the lowest wear intensity were obtained for the friction couple that consisted of the polymer and specimen denoted as A1; on the other hand, the highest friction coefficient and the highest wear were obtained for the friction couple that consisted of polymer and specimen denoted as B2. The results of the friction and wear investigation did not correlate with the composition of the ceramic element.

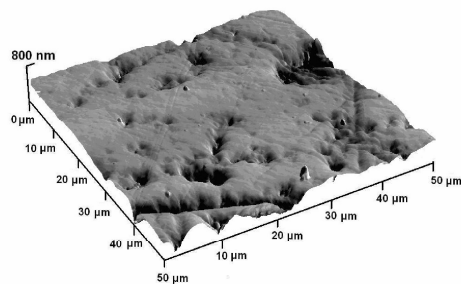
### 4. Results from 3D surface measurements

Three-dimensional surface analysis of ceramic specimens was performed by means of AFM before tribological tests. The obtained images were put in Fig. 3, by decreasing order of surface roughness.

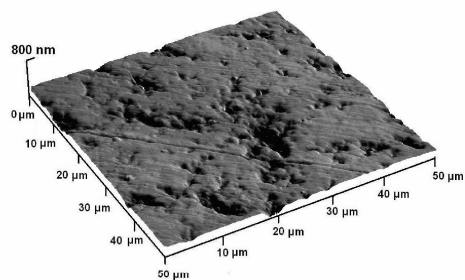
A1



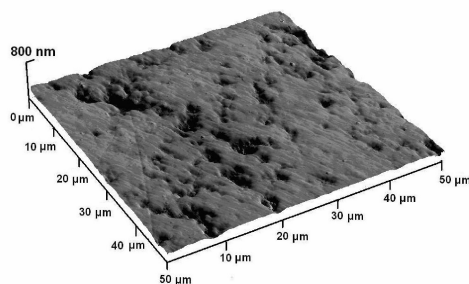
B1



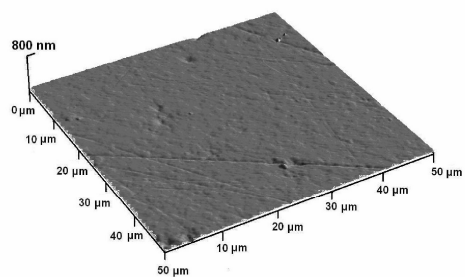
C



A2



D



B2

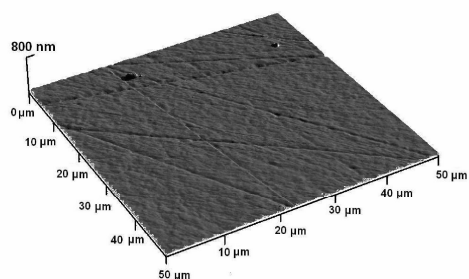


Fig. 3. The AFM images of investigated specimens ranked with decreasing roughness  
Rys. 3. Obrazy AFM badanych próbek, uszeregowane według malejącej chropowatości powierzchni

Using the AFM software measuring procedures, the 3D surface parameters of analysed specimens were determined and shown in Tab. 3.

Table 3. The average values ( $\bar{z}$ ) and standard deviation ( $\sigma$ ) of 3D surface roughness parameters of investigated ceramic plates

Tabela 3. Wartości średnie ( $\bar{z}$ ) i odchylenia standardowe ( $\sigma$ ) stereometrycznych parametrów chropowatości powierzchni badanych płytek ceramicznych

Specimen symbol	3D surface roughness parameters in nanoscale							
	R <sub>a</sub> [nm]		RMS [nm]		A [nm]		R <sub>z</sub> [nm]	
	$\bar{z}$	$\sigma$	$\bar{z}$	$\sigma$	$\bar{z}$	$\sigma$	$\bar{z}$	$\sigma$
A1	103.0	24,3	130.3	28	438.7	37.9	742.7	51.9
B1	77.0	21.7	101.7	27.4	440.3	53.5	728.3	65.0
C	26.3	1.5	36.0	2.0	275.0	71.5	345.0	75.4
A2	23.3	4.5	32	6.5	202.0	44.0	288.0	47.3
D	6.1	1.4	8.7	2.0	104.7	31.8	157.7	35.1
B2	5.4	0.2	7.8	0.1	71.3	4.7	154.0	40.2

The lowest values of surface roughness parameters, measured with nanoscale resolution, characterised specimen B2. The highest values of parameters, in fact, specimen A1 had the highest surface roughness. This is mostly an effect of the finishing method using rubbing disc with a higher granulation in the case of surface A1, and with a lower granulation in the case of surface B.

The kurtosis and skewness values of investigated ceramic plates are shown in Table 4.

Table 4. The average values ( $\bar{z}$ ) and standard deviation ( $\sigma$ ) of skewness and kurtosis of investigated ceramic plates

Tabela 4. Wartości średnie ( $\bar{z}$ ) i odchylenie standardowe ( $\sigma$ ) stereometrycznych miar zmienności i ostrości profilu powierzchni badanych płytek ceramicznych

Specimen symbol	The skewness and kurtosis values			
	S		K	
	$\bar{z}$	$\sigma$	$\bar{z}$	$\sigma$
A1	-0.89	0.22	0.75	1.05
B1	-1.35	0.37	1.39	2.72
C	-1.16	0.88	4.01	1.06
A2	-1.58	0.267	3.58	1.27
D	-1.86	0.07	11.19	3.04
B2	-1.40	0.60	10.53	3.95

All investigated specimens were characterised with skewness below zero, which indicates the advantage of the number of valleys. The trend of increasing profile sharpness together with roughness decrease (Kurtosis value above zero) was observed.

## 5. Discussion

Charts showing friction coefficient (Fig. 4) and wear intensity (Fig. 5) in a connection with RMS parameter describing the surface roughness were prepared on the basis of tribological tests results and surface roughness analysis of investigated materials.

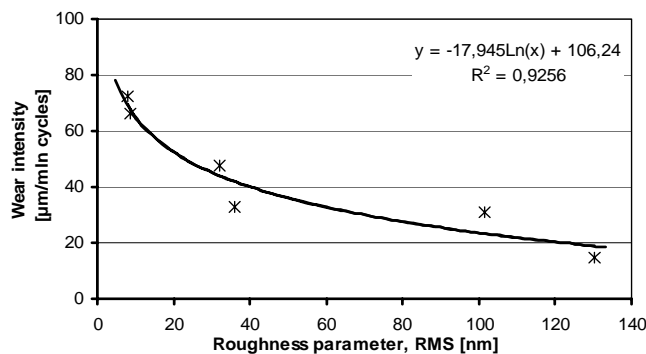


Fig. 4. The correlation of wear intensity and surface roughness parameter (RMS) of investigated materials with determined trend line, equation of regression and adjustment coefficient

Rys. 4. Wykres zależności intensywności zużywania od parametru chropowatości powierzchni (RMS) badanych materiałów, z wyznaczoną linią trendu, równaniem regresji oraz współczynnikiem dopasowania

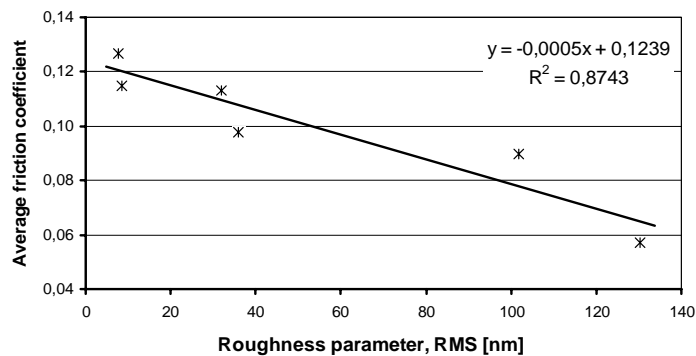


Fig. 5. The correlation of the friction coefficient and surface roughness parameter (RMS) of investigated materials with determined trend line, the equation of regression and adjustment coefficient

Rys. 5. Wykres zależności współczynnika tarcia od parametru chropowatości powierzchni (RMS) badanych materiałów, z wyznaczoną linią trendu, równaniem regresji oraz współczynnikiem dopasowania

Above-mentioned charts (Figs. 4 and 5) show that, in the case of ceramic-polymer friction, couples designed for endoprosthesis, the decrease of the surface roughness of ceramics is followed by an increase of wear intensity of the polymer element and an increase of the friction coefficient. The correlation of wear intensity and roughness is logarithmic, and the correlation of the friction coefficient and roughness are linear in the investigated range.

It is necessary to indicate that the friction process was followed by the deposition of polymer material on the ceramic plate. Fig. 6 shows the AFM image of the ceramic specimen with noticeable polymer deposit.

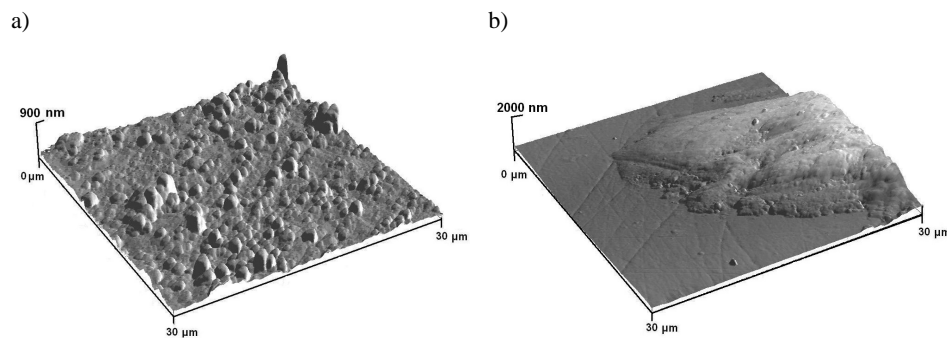


Fig. 6. The AFM images of polymer deposition on ceramic plates after the test:  
a) specimen A1 and b) specimen B2

Rys. 6. Obrazy AFM próbek ceramicznych z depozytem polimerowym po badaniu tribologicznym:  
a) próbka A1, b) próbka B2

In the ceramic-polymer friction joint, the smearing of polymer on the ceramic surface with high roughness is observed (Fig. 6a) – processes of moderate wear intensity. The micro-receptacles with Ringer solution (lubricant) are created in the valleys of high roughness surface, which counteracts the adhesion of the polymer to the specimen surface. On the other hand, on the ceramic surfaces with low roughness, there was observed adhesively bound large particles of polymer pulled out from the UHMWPE pin (Fig. 6b) – a process of high wear intensity.

Therefore, considering the wear of friction couple, the aim to obtain the lowest roughness of ceramic surface possible is unjustified.

## 6. Conclusions

In the case of materials with very low roughness, e.g.: ceramics, the use of standard profilometer is insufficient, due to mechanical filtration caused by the curvature radius of the gauge needle.

The roughness of hard ceramics affects the process of polymer transfer. In case of rough surfaces, polymer material is smeared on the ceramic surface creating a thin polymer film. As a result of this process, the wear and friction coefficients decrease. However, in the case of smooth ceramic surfaces, the strong adhesive bounds are created and some large particles of polymer are transferred to the ceramic surface. The result of this process is an increase of the wear and friction coefficients.

The conclusion from obtained tribological characteristics and results of surface parameters analysis by AFM is that, in the case of materials having very low roughness, the roughness decrease is followed by an increase of the friction coefficient, and the wear of polymer elements.

*Manuscript received by Editorial Board, April 02, 2008*

## References

- [1] Pytko S., Kowal A.: Implanty stawu biodrowego człowieka. Materiały Konferencji „Mechanika w Medycynie”. Rzeszów. 1998, p. 197-209.
- [2] Banchet V., Fidrici V., Abry J. C., Kapsa Ph.: Wear and friction characterization of materials for hip prosthesis. *Wear*, 263 (2007), pp.1066-1071.
- [3] Dowson D.: A comparative study of the performance of metallic and ceramic femoral head components in total replacement hip joint. *Wear* 190 (1995), p. 171-183.
- [4] Niemczewska M.: Kształtowanie powierzchni elementów endoprotez wykonanych z materiałów ceramicznych. Doctoral Thesis. Politechnika Krakowska. 2006.
- [5] www.emc-sa.pl, listopad 2007
- [6] Schreiner U., Simmacher M., Scheller G., Scharf G. P.: The influence of different surface treatment on the primary stability of cementless acetabular cups: an in vitro study. *Biomedizinische Technik. Biomedical Engineering*, 52 (2007), p. 243-247.
- [7] Liu X., Chu P. K., Ding C.: Surface modification of titanium, titanium alloys, and related materials for biomedical applications. *Materials Science and Engineering*, 47 (2004), p. 49-121.
- [8] Liu C., Bi Q., Matthews A.: Tribological and electrochemical performance of PVD TiN Coatings on femoral head of Ti-6Al-4V artificial hip joint. *Surface and Coatings Technology*, 163-164 (2003), p. 597-604.
- [9] Heinrich G., Grögler T., Rosiwal S. M., Singer R. F.: CVD diamond coated titanium alloys for biomedical and aerospace applications. *Surface and Coatings Technology*, 94-95 (1997), p. 514-520.
- [10] Traykova T., Aparicio C., Ginebra M. P., Planell J. A.: Bioceramics as nanomaterials. *Nanomedicine*, 1 (2006), p. 91-106.
- [11] Gawlik J., Niemczewska-Wójcik M., Piekoszewski W., Rozenberg O. A.: Precise surface machining of ceramic biomaterials. *Proc. of ICPM, Sandomierz-Kielce 2007*.
- [12] Piekoszewski W.: Identyfikacja warunków smarowania styku skoncentrowanego elementów chropowatych. Doctoral Thesis. Politechnika Poznańska. 1996.
- [13] Piekoszewski W.: Badania smarowanego styku skoncentrowanego elementów chropowatych. *Zagadnienia Eksploatacji Maszyn*. 34 (1999), p. 413-428.
- [14] Michalczewski R., Piekoszewski W., Szczerek M., Samborski T., Wasiak J.: Metoda i urządzenie do badań tribologicznych materiałów na endoprotezy. *Tribologia*. 5 (2002), p. 1491-1502.

- [15] Milošev I., Kosec T.: Metal ion release and surface composition of the Cu-18Ni-20Zn nickel-silver during 30 days immersion in artificial sweat. *Applied Surface Science*, 254 (2007), p. 644-652.
- [16] Kees M. G., Schlotterbeck H., Passemard R., Pottecher T., Diemunsch P.: Ringer solution: osmolarity and composition revisited. *Annales Françaises d'Anesthésie et de Réanimation*. 24 (2005), p. 653-655.
- [17] Ohmae N., Martin J.M., Mori S.: *Micro and Nanotribology*. ASME Press. New York 2005.

### **Analiza korelacji między parametrami 3D chropowatości powierzchni ceramicznej a charakterystykami tribologicznymi węzłów ceramiczno-polimerowych**

#### **Streszczenie**

Celem pracy było zbadanie korelacji między parametrami chropowatości powierzchni a charakterystykami tribologicznymi węzłów ceramiczno-polimerowych.

Badano trzpienie z UHMWPE trące w ruchu oscylacyjnym o płytki ceramiczne o różnej zawartości  $ZrO_2$  i  $Al_2O_3$ . Węzeł tarcia smarowany był płynem Ringera. Badania prowadzono z użyciem tribotestera T-17. Wykonano pomiary współczynnika tarcia i intensywności zużywania elementów węzła tarcia.

Powierzchnia próbek badana była za pomocą mikroskopu sił atomowych (AFM).

W efekcie przeprowadzonych badań stwierdzono, że stan powierzchni twardych materiałów ceramicznych wpływa na rodzaj zużywania współpracującego polimeru. W przypadku ceramiki o dużej chropowatości dochodzi do wytworzenia filmu polimerowego na powierzchni ceramiki na skutek namazywania, a w konsekwencji następuje obniżenie współczynnika tarcia i zmniejszenie zużycia. Natomiast w przypadku ceramiki o niskiej chropowatości tworzą się szpewienia adhezyjne ceramika-polimer, a w rezultacie następuje odrywanie dużych fragmentów polimeru, tym samym wzrost współczynnika tarcia i zużycia.

